Base-Pair Mismatch Can Destabilize Small DNA Loops through Cooperative Kinking

Jiyoun Jeong and Harold D. Kim*
School of Physics, Georgia Institute of Technology, 837 State Street, Atlanta, Georgia 30332-0430, USA

(Received 4 January 2019; published 29 May 2019)

Base-pair mismatch can relieve mechanical stress in highly strained DNA molecules, but how it affects their kinetic stability is not known. Using single-molecule fluorescence resonance energy transfer, we measured the lifetimes of tightly bent DNA loops with and without base-pair mismatch. Surprisingly, for loops captured by stackable sticky ends which leave single-stranded DNA breaks (or nicks) upon annealing, the mismatch decreased the loop lifetime despite reducing the overall bending stress, and the decrease was largest when the mismatch was placed at the DNA midpoint. These findings suggest that base-pair mismatch increases bending stress at the opposite side of the loop through an allosteric mechanism known as cooperative kinking. Based on this mechanism, we present a three-state model that explains the apparent dichotomy between thermodynamic and kinetic stability.

DOI: 10.1103/PhysRevLett.122.218101

Cellular DNA is constantly exposed to the possibility of mispairing (i.e., noncomplementary base pairing) [1]. Most commonly, mismatched base pairs result from base misincorporation during gene replication [2] and heteroduplex formation between slightly different DNA sequences during homologous recombination [3]. They can also arise from exposure to DNA damaging agents that modify nucleobases [4,5]. Because of less favorable base pairing and stacking [6], mismatched base pairs can increase local flexibility of double-stranded DNA [7–9], and, consequently, the capture rate of tightly bent loops [10]. For example, 1- to 3-bp mismatch near the center of a short DNA fragment (<150 bp) was shown to increase the rate of DNA loop formation by 1 to 2 orders of magnitude [11,12]. The kinetics of loop formation or capture is intuitively understood by a one-dimensional free energy curve with the end-to-end distance as a single reaction coordinate [Fig. 1(a)]. Base-pair mismatch would reduce the mechanical work required to bring two distant DNA sites to proximity; all the more so for a shorter end-to-end distance. Therefore, the base-pair mismatch would lower the transition state relative to the unlooped state [dotted line, Fig. 1(a)].

Base-pair mismatch is also expected to affect the breakage or release rate of small DNA loops that are captured by protein complexes [13] or by sticky ends of the DNA itself [14]. Looped DNA segments substantially shorter than one persistence length are subject to a high level of mechanical stress; therefore, the free energy of the looped state is significantly lowered in the presence of the mismatch. According to the free energy diagram in Fig. 1(a), the transition state, being at a slightly longer end-to-end distance by $\Delta x^{\ddagger}$, would be lowered to a lesser degree [Fig. 1(a)]. Therefore, the one-dimensional model predicts that the rate of loop release would decrease in the presence of base-pair mismatch.

Such a prediction of mismatch dependence seems plausible considering the success of the model in predicting the length dependence of loop capture and release rates [15,16]. In the length regime where the free energy of loop formation is dominated by bending energy, increasing DNA length effectively reduces the tilt in the free energy curve because states at shorter end-to-end distances receive more stress relief, similar to the dotted line in Fig. 1(a). This change predicts that loop capture and release rates measured at different DNA lengths would be anticorrelated; loops associated with higher mechanical stress are captured more slowly and released more quickly. This prediction has been confirmed for both DNA loops captured by *lac* repressor [15] and DNA loops captured by sticky ends [17,18]. While increasing DNA length evens out the bending stress over the entire DNA molecule, the base-pair mismatch tends to localize sharp bending. Therefore, the effect of base-pair mismatch might be quite different from that of increasing DNA length.

In this Letter, we investigated how base-pair mismatch affects the stability of small DNA loops. As a model system for DNA loop capture and release, we used short double-stranded DNA molecules with sticky ends. To monitor loop capture and loop release events, we used the single-molecule fluorescence resonance energy transfer (FRET) assay as previously published [12,14]. Briefly, DNA molecules labeled with Cy3 and Cy5 near their sticky ends were immobilized to a NeutrAvidin-coated glass surface through a biotin linker. Such a surface attachment scheme is expected to slightly lower the loop capture rate [19,20], but this effect is irrelevant to the current study. Loop capture or release was triggered by the exchange of buffers with different NaCl concentrations

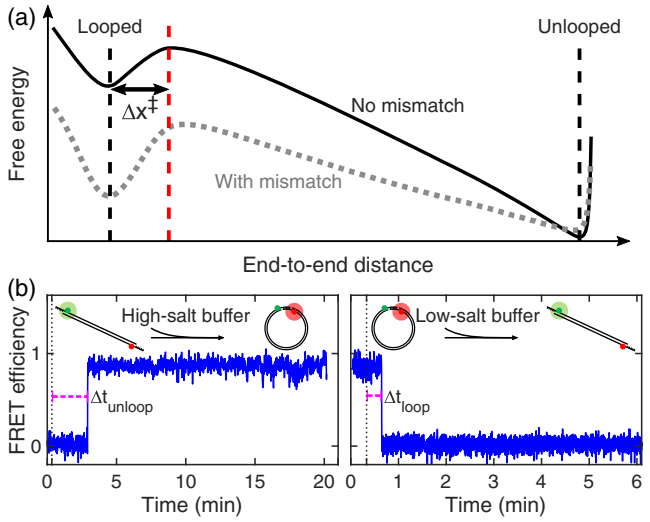

FIG. 1. (a) Schematic illustration of a free energy landscape for DNA loop capture and release. The two minimum free energy states correspond to the looped and unlooped states (vertical black lines). The transition state (vertical red line) is separated from the looped state by a small distance $\Delta x^{\ddagger}$, which is equal to the capture radius. The base-pair mismatch is expected to increasingly untilt the solid curve toward shorter end-to-end distances, which results in the dotted curve. (b) Typical FRET trajectories of a DNA molecule undergoing loop capture (left) and loop release (right). The DNA molecule labeled with Cy3 (green) and Cy5 (red) is in the low FRET state when unlooped, and in the high FRET state when looped. A sudden increase or decrease in NaCl concentration at the 20-s time point (marked by a vertical dotted line) triggers the transition.

(see Supplemental Material [21] for more details). The first transition times (Δt) in the FRET signals [Fig. 1(b)] of ~150 individual DNA molecules were collected. The mean of Δt spent in the unlooped state before looping is defined as the loop capture time (τ_{unloop}), and the mean of Δt spent in the looped state before unlooping is defined as the loop release time or loop lifetime (τ_{loop}). All DNA molecules used in this study were shorter than 150 bp, the length regime where the free energy of loop formation is dominated by bending energy.

We first tried the loop capture geometry used in DNA cyclization, which we term as the "hairband loop" [Fig. 2(a)]. In this geometry, the complementary overhangs protrude from different strands so that the sticky ends can anneal in trans and stack upon each other. In a previous study, we showed that this end stacking, or equivalently nick closing, substantially increases the hairband loop stability [22]. Using the single-molecule FRET assay, we measured the hairband loop capture times with and without base-pair mismatch in the center. As shown in Fig. 2(b), hairband loop capture took less time in the presence of the mismatch as expected. The loop capture time further decreased with increasing mismatch size [circles, Fig. 2(b)]. The base-pair mismatch in the center position led to the largest decrease in the loop capture time, and the decrease dropped as the mismatch was placed further from the center [triangles, Fig. 2(b)]. These observations confirm previous findings that mismatched base pairs reduce the energy barrier for loop formation by increasing DNA bendability [8,11,27,28], and this barrier reduction is most effective when the mismatch is in the center [29].

Next, we measured the hairband loop release times or loop lifetimes (τ_{loop}) with and without the mismatch in the center. Since a mismatch could relieve the bending stress of the hairband loop, we thought that the loop lifetime would become longer. To our surprise, we observed the exact opposite effect where the central mismatch decreased the hairband loop lifetime [Fig. 2(c)]. Increasing the size of the mismatch from 1 to 3 bp led to a further decrease in the lifetime. This effect seemed to plateau past the mismatch size of 3 bp [Fig. 2(c)]. This result suggests that the mismatch-containing hairband loop is more kinetically unstable than the mismatch-free loop, which seems paradoxical through the lens of the one-dimensional model presented in Fig. 1(a).

We thus considered the possibility that the transition state depends on other reaction coordinates besides the end-to-end distance, such as the closing angles at the loop junction. Since base stacking at the nick(s) in the hairband loop is a key determinant of decyclization kinetics [22], we asked whether the central mismatch could destabilize the hairband loop by allosterically inducing the nick opening. To investigate such allosteric coupling, we calculated the curvature profile of a kinkable semiflexible loop [23] containing a defect with zero rigidity from a Monte Carlo simulation (see Supplemental Material [21] for details). As shown in Fig. 2(d), a kink with a sharp bending angle appeared most frequently at the farthest end of the loop from the defect. We also calculated the minimum energy conformation of a semiflexible loop while varying the rigidity of the defect and found that the bending angles of farthest points were highly correlated [Fig. 2(e)]. Since kinking at one site increases the probability of kinking at its antipodal site, the phenomenon is reminiscent of positive cooperativity and is thus termed cooperative kinking [30]. Such an effect has been observed in torsionally strained DNA minicircles by cryoelectron microscopy and molecular dynamics simulations [30–32].

We hypothesized that the enhanced flexibility of the central mismatch destabilizes the hairband loop preventing nicks(s) on the opposite side from closing. This hypothesis provides a few testable predictions. First, if the mismatch were displaced from the midpoint of the DNA, the degree of destabilization would be dampened. In agreement with this prediction, we observed a longer loop lifetime when the mismatch was placed at a quarterpoint instead of the center [Fig. 2(f)]. Second, the cooperative kinking hypothesis requires nicks that can buckle under the bending stress, and therefore the mismatch-induced destabilization would be

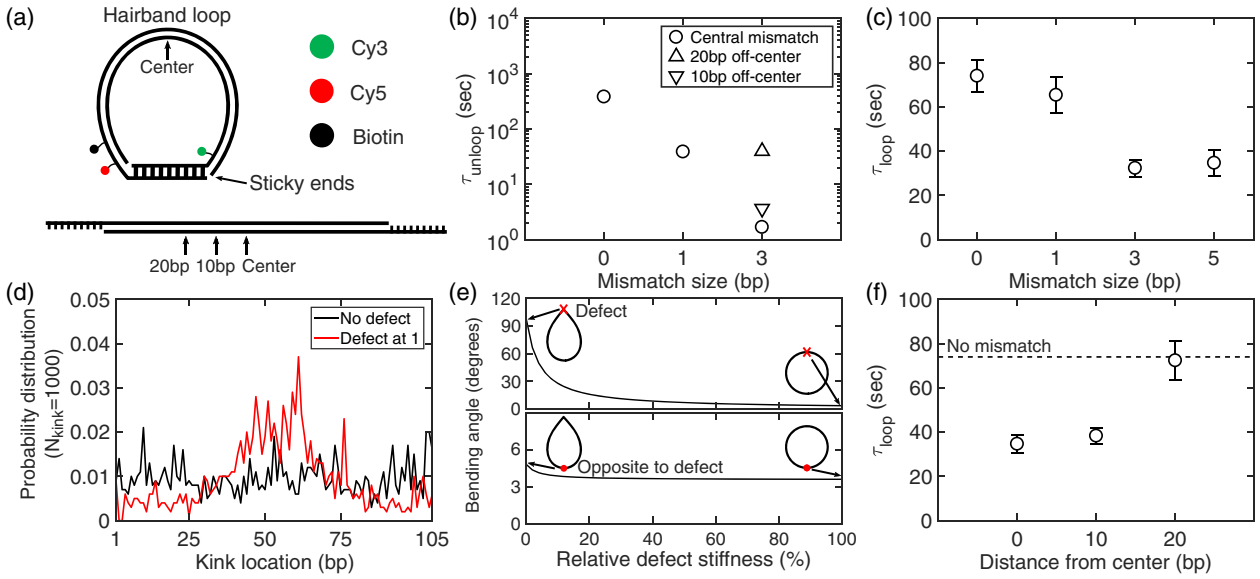

FIG. 2. (a) Schematic of a hairband loop captured by sticky ends. The schematic on top shows base-paired overhangs, Cy3 (green circle), Cy5 (red circle), and the biotin linker (black circle). In this geometry, the overhangs on opposite strands form a duplex that can stack at both nicks of the loop. Different positions of base-pair mismatch tested in our experiments are marked on the linear form at the bottom. Only the bases on the overhangs are shown. (b) Measured loop capture time of the hairband molecules (108 bp) as a function of the central mismatch size (circles). Experimental data with an off-center 3-bp mismatch are also shown as triangles. The upright and flipped triangles represent the loop capture times for base-pair mismatches placed at 20 and 10 bp away from the center of the molecule, respectively. Error bars, the standard errors of the mean, are smaller than the size of the symbols. (c) Measured hairband loop lifetime (loop release time) as a function of the central mismatch size. Error bars represent the standard errors of the mean. (d) Probability distribution of kink positions obtained by Monte Carlo simulations of coarse-grained circular DNA of 105 bp in size. A kink appears uniformly along the contour of the DNA circle when there is no preexisting flexible defect (black). In contrast, the presence of a preexisting defect at the first base-pair biases the probability distribution of kink positions (red). (e) Bending angle calculated from the minimum-energy conformation of a DNA minicircle (105 bp) with a defect. Top and bottom figures show bending angles at the defect and the site opposite to the defect, respectively, as a function of the defect stiffness relative to an intact base pair. The minimum-energy conformations of the two extreme cases of the defect stiffness (0% and 100%) are also shown along the curves with the defect position marked by *X*. (f) Measured hairband loop lifetime as a function of the mismatch position (3 bp in size). For comparison, the horizontal dotted line shows the loop lifetime without the mismatch. Error bars represent the standard errors of the mean.

eliminated in a loop capture geometry free of end stacking. We thus tested a different loop geometry referred to as the "hairpin loop," where the complementary overhangs protrude from the same strand [Fig. 3(a)]. In this geometry, the sticky ends anneal in *cis* and cannot stack upon each other. Using these new DNA constructs with a central mismatch of various sizes, we repeated loop capture and release experiments. Similar to hairband loop capture, the hairpin capture time decreased with the size of base-pair mismatch [Fig. 3(b)]. However, in sharp contrast to the hairband loop, the hairpin loop lifetime increased with mismatch size [Fig. 3(c)]. The effect of the base-pair mismatch on the hairpin loop stability is therefore consistent with the prediction of the one-dimensional model. Overall, the lifetimes of hairpin loops were shorter than those of hairband loops, which is consistent with the easier rupture of the DNA duplex in an unzipping geometry than in a shearing geometry [33–35]. These results lend strong support to the idea that cooperative kinking governs the kinetic stability of a mismatch-containing hairband loop.

The mismatch dependence of the hairband loop release kinetics reveals the limitations of the one-dimensional two-state model [Fig. 1(a)] and invites us to consider additional states and alternative reaction paths along another dimension. Here, we present two different paths ($k^{(0)}$ and $k^{(m)}$) that are likely to be the dominant ones for mismatch-free and mismatch-containing DNA [Fig. 4(a)]. Each path goes through three different states: unlooped, unstacked, and stacked. The loop capture rate is much greater in the presence of a central mismatch due to its enhanced flexibility ($k_1^{(m)} \gg k_1^{(0)}$). The reverse rate is expected to be slower with the mismatch ($k_2^{(m)} < k_2^{(0)}$) because of the weaker loop tension. Mismatch-free DNA undergoes small bending fluctuations uniformly throughout its contour, and therefore, follows an arclike trajectory toward the looped state where end stacking (nick closing) and end unstacking (nick opening) transitions may occur. In comparison, DNA with a mismatch in the center can be sharply bent at a much lower energy cost, and therefore, the most dominant path toward the looped state will resemble a tweezerslike

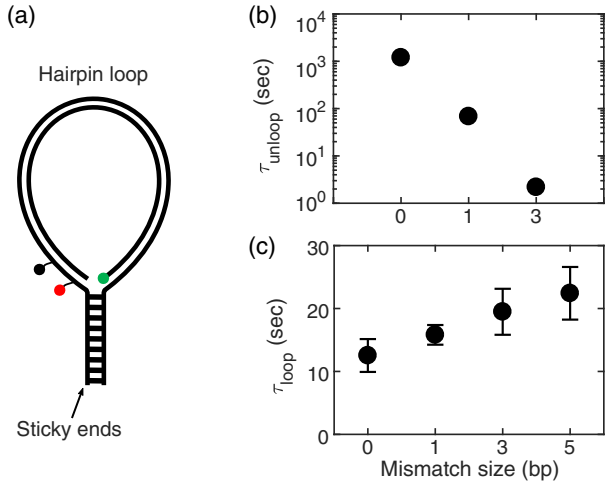

FIG. 3. (a) Schematic of a hairpin loop. The schematic shows the FRET pair (green and red circles), the biotin linker (black circle), and base-paired overhangs. In this geometry, the overhangs on the same strand form a duplex like a zipper. (b) Loop capture time of the hairpin (105 bp) molecules as a function of the central mismatch size. Error bars are omitted due to their small sizes. (c) Hairpin loop lifetime as a function of the central mismatch size. Error bars represent the standard errors of the mean.

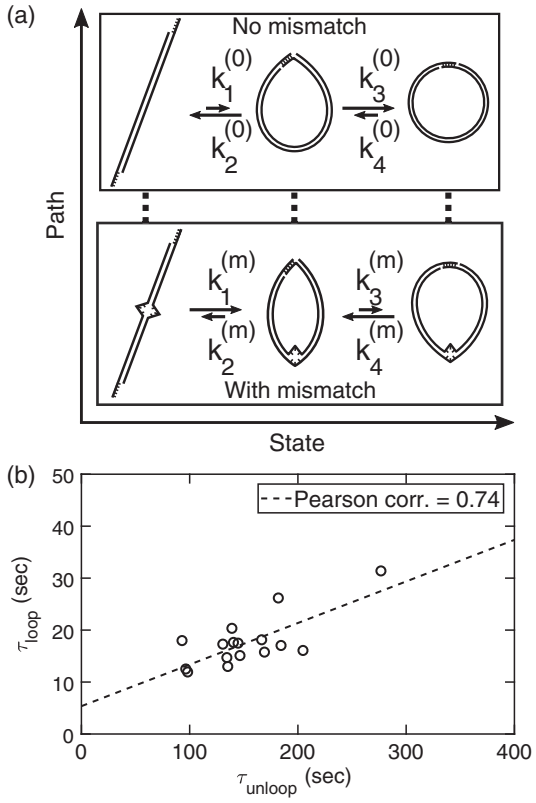

FIG. 4. (a) The three-state model for hairband loop closure and release. The three states from left to right are unlooped, unstacked, and stacked states. The looped state is a mixed state between the unstacked and stacked states. Therefore, the apparent loop capture rate (k_{loop}) is equal to k_1, but the apparent loop release rate (k_{unloop}) depends on k_2, k_3, and k_4. For the hairpin loop, $k_3 = 0$, and therefore, k_{unloop} is equal to k_2. Two representative paths for central mismatch size 0 and m are highlighted with arclike (top) and tweezerslike (bottom) motions, respectively. The vertical dotted lines imply the continuum of paths running parallel to the two extreme ones shown. (b) Correlation between loop capture and release times of 16 unrelated hairband DNA molecules of the same size (94 bp). The correlation coefficient between the two lifetimes is 0.74 and a 95% confidence interval is between 0.25 and 0.96. The loop capture and release times were measured in equilibrium (i.e., no buffer exchange) at a slightly elevated temperature of 34 °C with [NaCl] = 700 mM.

motion. As a result of this motion, the sticky ends anneal at a sharp angle, and the hairband loop with the mismatch faces a higher energy barrier for end stacking (nick closing) than without ($k_3^{(m)} \ll k_3^{(0)}$). The mismatch not only suppresses end stacking, but also promotes end unstacking (nick opening) through cooperative kinking, which implies $k_4^{(m)} \gg k_4^{(0)}$. Hence, the apparent release rate of the hairband loop (k_{unloop}) becomes faster with the mismatch than without because the looped state with the mismatch is heavily biased towards the unstacked state. In comparison, for the hairpin loop that cannot proceed to the stacked state, the three-state model is reduced to the two-state model, and the loop release rate is slower with the mismatch ($k_2^{(m)} < k_2^{(0)}$).

The two paths boxed in Fig. 4(a) represent the two most extreme paths in terms of kinetics, the top path for the slowest hairband loop capture and release, and the bottom for the fastest. In reality, there exists a continuum of paths going through the three states with intermediate rates, and the flexibility profile of DNA determines the relative weights at which individual paths are taken. Therefore, any changes to the flexibility profile of DNA would lead to correlated changes in the hairband loop capture and release rates. To test this idea, we measured hairband loop capture and release times of 16 unrelated sequences, all of the same length. The measured times are scattered over a threefold range [Fig. 4(b)], indicative of sequence-dependent bending rigidity of short DNA [36]. Although limited in sample size, we observed a significant degree of correlation between the two times with a Pearson correlation of 0.74 [Fig. 4(b)] and a 95% confidence interval of this correlation was estimated to be between 0.25 and 0.96 by bootstrap resampling (see Supplemental Material [21] for details). In line with our observation, six different DNA molecules studied recently by Jang *et al.* [20] also show a strong correlation between hairband loop capture and release times. These findings suggest that cooperative kinking is a general mechanism that governs the kinetics of hairband loop capture and release.

In conclusion, our results suggest that base-pair mismatch can constrain the geometry of DNA loops captured

by sticky ends through cooperative kinking, and the close coupling between hairband loop geometry and end stacking can give rise to correlated changes between loop capture and release times ("easy come, easy go"). We propose a three-state model that correctly describes the effect of mismatched base pairs on the apparent kinetics of loop capture and release. Although this allosteric effect of mismatched base pairs on DNA loop stability is inferred from a particular DNA loop geometry with stackable ends, it could still be applicable to protein-mediated DNA loops in light of the role of DNA curvature in DNA-protein interactions [37,38]. In a real biological context, the effect is likely to be more complex because of the diversity in loop capture geometry [39]. Beyond passively captured DNA loops, it would be interesting to investigate whether base-pair mismatches can also influence the kinetics of DNA loop extrusion [40,41] through cooperative kinking.

This work was supported by National Institutes of Health (Grant No. R01GM112882) and National Science Foundation (Grant No. 1517507). We thank the members of the Kim laboratory for critical discussions and helpful comments.

*Corresponding author.
harold.kim@physics.gatech.edu

[1] N. Chatterjee and G. C. Walker, Environmental and molecular mutagenesis **58**, 235 (2017).
[2] T. A. Kunkel and D. A. Erie, Annu. Rev. Genet. **49**, 291 (2015).
[3] K.-C. Tham, R. Kanaar, and J. H. G. Lebbink, DNA Repair **38**, 75 (2016).
[4] J. Cadet and J. R. Wagner, Cold Spring Harbor Perspect. Biol. **5**, a012559 (2013).
[5] A. Granzhan, N. Kotera, and M.-P. Teulade-Fichou, Chem. Soc. Rev. **43**, 3630 (2014).
[6] J. SantaLucia and D. Hicks, Annu. Rev. Biophys. Biomol. Struct. **33**, 415 (2004).
[7] G. Rossetti, P. D. Dans, I. Gomez-Pinto, I. Ivani, C. Gonzalez, and M. Orozco, Nucleic Acids Res. **43**, 4309 (2015).
[8] M. Sharma, A. V. Predeus, S. Mukherjee, and M. Feig, J. Phys. Chem. B **117**, 6194 (2013).
[9] S. Chakraborty, P. J. Steinbach, D. Paul, H. Mu, S. Broyde, J.-H. Min, and A. Ansari, Nucleic Acids Res. **46**, 1240 (2018).
[10] A. Dittmore, S. Brahmachari, Y. Takagi, J. F. Marko, and K. C. Neuman, Phys. Rev. Lett. **119**, 147801 (2017).
[11] J. D. Kahn, E. Yun, and D. M. Crothers, Nature (London) **368**, 163 (1994).
[12] R. Vafabakhsh and T. Ha, Science **337**, 1097 (2012).
[13] C. Tardin, Biochimie **142**, 80 (2017).
[14] J. Jeong, T. T. Le, and H. D. Kim, Methods **105**, 34 (2016).
[15] Y.-J. Chen, S. Johnson, P. Mulligan, A. J. Spakowitz, and R. Phillips, Proc. Natl. Acad. Sci. U.S.A. **111**, 17396 (2014).
[16] P. J. Mulligan, Y.-J. Chen, R. Phillips, and A. J. Spakowitz, Biophys. J. **109**, 618 (2015).
[17] T. T. Le and H. D. Kim, Biophys. J. **104**, 2068 (2013).
[18] T. T. Le and H. D. Kim, Nucleic Acids Res. **42**, 10786 (2014).
[19] J. T. Waters and H. D. Kim, Macromolecules **46**, 6659 (2013).
[20] Y. Jang, H. Son, S.-W. Lee, W. Hwang, S.-R. Jung, J. A. W. Byl, N. Osheroff, and S. Lee, Cell Chem. Biol. **26**, 502 (2019).
[21] See Supplemental Material at http://link.aps.org/supplemental/10.1103/PhysRevLett.122.218101 for more details on the materials, experimental methods, and simulation procedures, which includes Refs. [18,22–26].
[22] J. Jeong and H. D. Kim, https://doi.org/10.1101/503490.
[23] A. Vologodskii and M. D. Frank-Kamenetskii, Nucleic Acids Res. **41**, 6785 (2013).
[24] T. T. Le and H. D. Kim, J. Visualized Exp. **88**, e51667 (2014).
[25] C. E. Aitken, R. A. Marshall, and J. D. Puglisi, Biophys. J. **94**, 1826 (2008).
[26] X. Zheng and A. Vologodskii, Biophys. J. **96**, 1341 (2009).
[27] K. A. Schallhorn, K. O. Freedman, J. M. Moore, J. Lin, and P. C. Ke, Appl. Phys. Lett. **87**, 033901 (2005).
[28] C. Yuan, E. Rhoades, X. W. Lou, and L. A. Archer, Nucleic Acids Res. **34**, 4554 (2006).
[29] P. Ranjith, P. B. S. Kumar, and G. I. Menon, Phys. Rev. Lett. **94**, 138102 (2005).
[30] T. A. Lionberger, D. Demurtas, G. Witz, J. Dorier, T. Lillian, E. Meyhfer, and A. Stasiak, Nucleic Acids Res. **39**, 9820 (2011).
[31] R. N. Irobalieva, J. M. Fogg, D. J. Catanese Jr, T. Sutthibutpong, M. Chen, A. K. Barker, S. J. Ludtke, S. A. Harris, M. F. Schmid, W. Chiu *et al.*, Nat. Commun. **6**, 8440 (2015).
[32] T. Sutthibutpong, C. Matek, C. Benham, G. G. Slade, A. Noy, C. Laughton, J. P. K. Doye, A. A. Louis, and S. A. Harris, Nucleic Acids Res. **44**, 9121 (2016).
[33] M. Mosayebi, A. A. Louis, J. P. K. Doye, and T. E. Ouldridge, ACS Nano **9**, 11993 (2015).
[34] J. Zhang, Y. Yan, S. Samai, and D. S. Ginger, J. Phys. Chem. B **120**, 10706 (2016).
[35] S. R. Tee and Z. Wang, ACS Omega **3**, 292 (2018).
[36] M. Zuiddam and H. Schiessel, Phys. Rev. E **99**, 012422 (2019).
[37] R. Rohs, S. M. West, A. Sosinsky, P. Liu, R. S. Mann, and B. Honig, Nature (London) **461**, 1248 (2009).
[38] T. Zhou, N. Shen, L. Yang, N. Abe, J. Horton, R. S. Mann, H. J. Bussemaker, R. Gordân, and R. Rohs, Proc. Natl. Acad. Sci. U.S.A. **112**, 4654 (2015).
[39] A. R. Haeusler, K. A. Goodson, T. D. Lillian, X. Wang, S. Goyal, N. C. Perkins, and J. D. Kahn, Nucleic Acids Res. **40**, 4432 (2012).
[40] M. Ganji, I. A. Shaltiel, S. Bisht, E. Kim, A. Kalichava, C. H. Haering, and C. Dekker, Science **360**, 102 (2018).
[41] J. F. Marko, P. De Los Rios, A. Barducci, and S. Gruber, https://doi.org/10.1101/325373.